A R C H I V E O F M E C H A N I C A L E N G I N E E R I N G

VOL. LXI 2014 Number 3

10.2478/meceng-2014-0025

Key words: rotodynamic pumps, radial thrust, pumps with single volutes, affinity laws, measurement of radial forces

KRZYSZTOF KARAŚKIEWICZ [*], *MAREK SZLAGA* [**]

EXPERIMENTAL AND NUMERICAL INVESTIGATION OF RADIAL FORCES ACTING ON CENTRIFUGAL PUMP IMPELLER

The paper presents the results of measurements and predictions of radial thrust in centrifugal pump with specific speed n_s = 26. In the pump tested, a volute with rectangular cross-section was used. The tests were carried out for several rotational speeds, including speeds above and below the nominal one. Commercial code ANSYS Fluent was used for the calculations. Apart from the predictions of the radial force, the calculations of axial thrust were also conducted, and correlation between thrust and the radial force was found. In the range of the measured rotational speeds, similarity of radial forces was checked.

1. Introduction

The knowledge of force acting on rotor is essential to correctly select bearings in centrifugal pump and to decide whether a balancing device should, or should not be used.

When a balancing device for axial force is necessary, predicting the accurate value of axial force F_a (eq. 1) is important. When balancing disk is used, the whole axial force must be balanced, and in the case of using a balancing drum – nearly 85% of it.

$$F_a = \int_{r''}^{r_2}\int_0^{2\pi} p_{II}(r,\phi) r dr d\phi - \int_{r'}^{r_2}\int_0^{2\pi} p_I(r,\phi)\, r dr d\phi \pm \sum F_{remaining} \qquad (1)$$

For too high radial force, one should consider a double volute instead of single volute.

[*] *Warsaw University of Technology, Institute of Heat Engineering, ul. Nowowiejska 25, 00-665 Warsaw, Poland; E-mail: krzysztof.karaskiewicz@meil.pw.edu.pl*

[**] *Powen-WafaPomp, Dept. of Research and Development, ul. Odlewnicza 1, 03-231 Warsaw, Poland; E-mail: marek.szlaga@powen.com.pl*

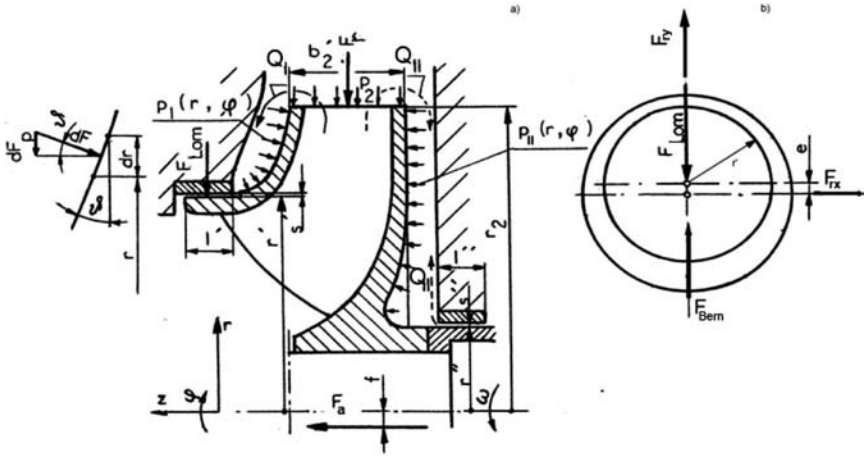

Fig. 1. Pressures and forces acting on rotor external surfaces

The components x and y of radial force depend on pressure distribution around the impeller.

$$F_{rx} = \int_{r'}^{r_2} \int_{0}^{2\pi} p_I(r,\phi) \operatorname{tg}\vartheta \cos\phi r dr d\phi + \int_{0}^{2\pi} p_2(\phi) b_2' r_2 \cos\phi d\phi \tag{2}$$

$$F_{ry} = \int_{r'}^{r_2} \int_{0}^{2\pi} p_I(r,\phi) \operatorname{tg}\vartheta \sin\phi r dr d\phi + \int_{0}^{2\pi} p_2(\phi) b_2' r_2 \sin\phi d\phi \tag{3}$$

where total radial force $F_r = \sqrt{F_{rx}^2 + F_{ry}^2}$.

The radial force, called sometimes the radial thrust, depends on head and diameter of the impeller. Taking into account the fact that the pump head is a quadratic function of a rotational speed, and knowing the impeller diameter, this force can be described as:

$$F_r \sim Hdb \sim n^2 d^3 b \tag{4}$$

This force reaches high values in high-speed pumps or pumps with large impeller diameters. Its value is influenced also by the type of casing (single volute, double volute, diffuser) and does a pump operate at the BEP or not. The radial thrust reaches the highest values in single volute pumps at duty points far from the BEP. A pump operating outside acceptable flow range can suffer from bearing problems or even shaft breaking [1].

Pump designers readily refer to simple empirical formulas. The earliest one, based on one size of the pump only, was proposed by Stepanoff [2].

Agostinelli et al. [3] measuring radial thrust for sixteen different pumps extended the formula involving the effect of specific speed on radial force. Biheller [4] and the Hydraulic Institute [5] proposed some other relationships as well. The values obtained by the HI were over-predicted for low specific speeds compared to those found by Agostinelli [3]. Later, the Hydraulic Institute corrected its values [6], so they comply well with the Agostinelli's ones [3]. The direction of the radial thrust cannot be found from theses relations.

In this paper, results of experimental and numerical investigations are presented for centrifugal pump with the rectangular cross-section volute.

2. Pump test-bed

The tests were carried out on the test-bed presented in Fig. 2. The pump (3) with exchangeable impellers was the essential part of the test bed. In the tests, the impeller of specific speed n_s = 26 was used. The pump sucked water from tank (1) and delivered it to the same tank. Pressures before (4) and after (5) the pump, flow rate (6), rotational speed (7), torque (8) and radial force (11) were measured on the test-bed.

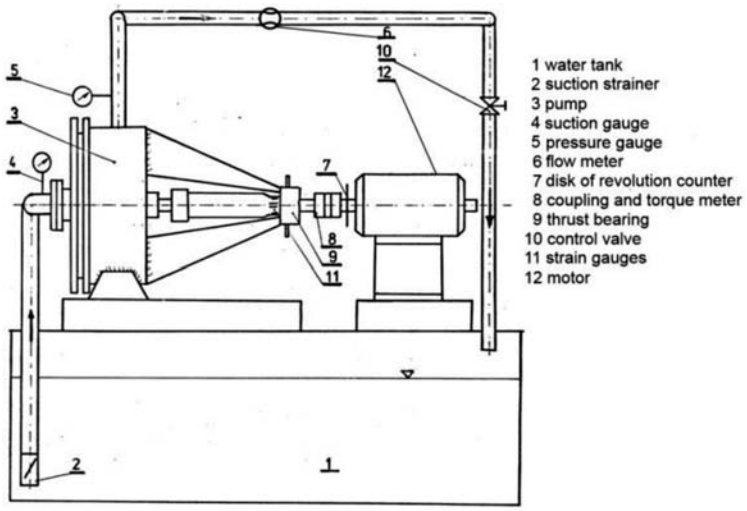

Fig. 2. Pump test-bed

Volute casing of rectangular cross-section (Fig. 3) was made of wood, so it was easy to change its dimensions. In the presented investigations, the inlet volute width was b_3 = 40 mm and was equal to the volute casing width b_4. The width of the impeller outlet together with the shrouds was b_2 = 34 mm and its diameter d_2 = 264 mm.

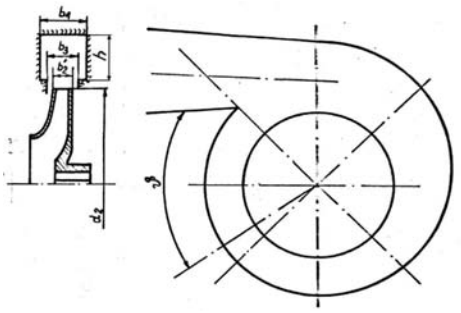

b_4 – volute casing width

b_3 – inlet volute width

b_2 – impeller outlet width including shrouds

d_2 – impeller diameter

Fig. 3. The volute casing of the pump tested

The radial force was measured with strain gauges attached to the shaft (p. 11 in Fig. 2). For calibration procedure, the shaft was lengthened to apply standard force G (Fig.4). In this way the calibration curve was determined. The radial force F was calculated from the relationship (a = 310 mm, b = = 200 mm, c = 640 mm)

$$F = G\frac{a+b+c}{a+b} = 2.25G$$

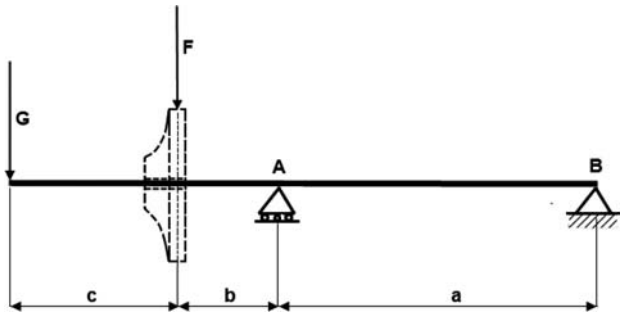

Fig. 4. Schematic diagram of radial force F calibration

The investigations and predictions cover rotational speeds of n = 1150, 1300, 1450, 1600 rpm for one volute casing.

3. Results of measurements and numerical predictions

The commercial code ANSYS Fluent was employed for numerical predictions of hydraulic forces acting on impeller. The grid covering the flow area consisted of $8.8 \cdot 10^5$ nodes. Figure 5 shows the 3D pump model with inlet part, impeller, volute and outlet channel and the corresponding grid.

For calculations, we used the standard turbulence k-ε model. The predictions covered rotational speeds of n = 1300, 1450, 1600 rpm.

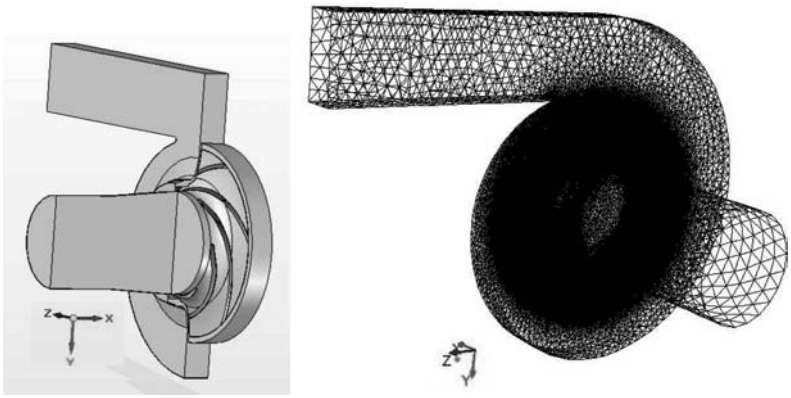

Fig. 5. The pump model with corresponding grid

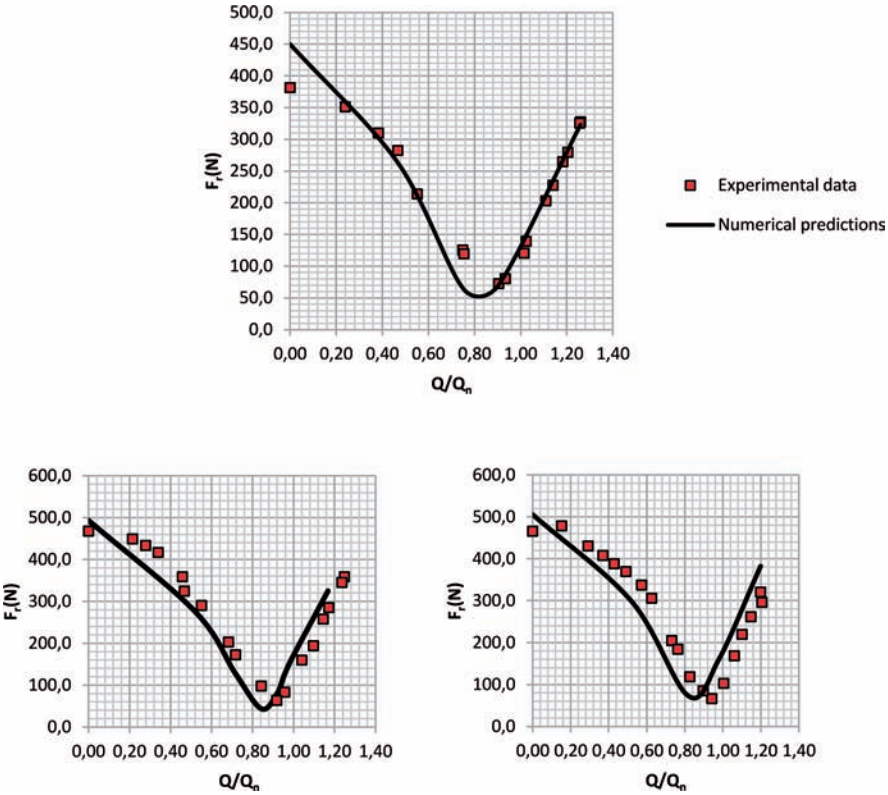

Fig. 6. Experimental and numerical investigations for: a) n = 1300 rpm; b) n = 1450 rpm; c) n = 1600 rpm

The predictions are generally in accordance with the measurements. The value of radial thrust for rotational speed n = 1300 rpm at shut off flow $Q = 0$ is over-predicted, but the shape of the radial force curve is very similar to that determined by the measurements.

Figure 7 shows direction of both measured and predicted radial force. The calculated results don't coincide well with measurements, however, satisfactory agreement was achieved between the magnitudes of experimental and calculated radial force. The calculations were made using the frozen rotor approach with one impeller blade positioned against the tongue, which might have some influence on the pressure field between the rotor and the volute.

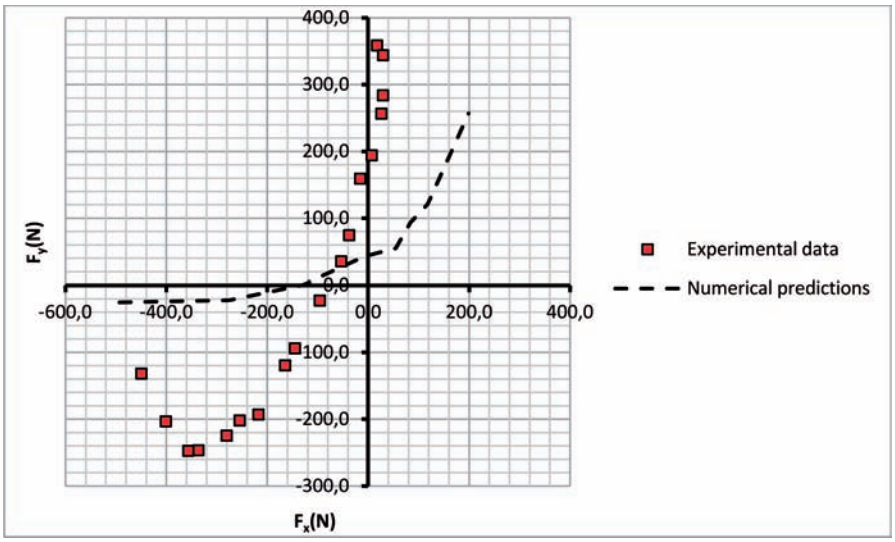

Fig. 7. The direction of radial force for n = 1450 rpm

The frozen rotor scheme supports steady-state prediction in the local frame of reference on each side of the interface. This scheme is used for non-symmetric flow domain of volute. The relative circumferential position of the impeller with respect to the volute tongue is fixed in time. In this case, the solution provides a snapshot of the flow regime. The predictions thus depend on the rotor position, so one can obtain inadequate results for local flow fields.

The advantages of the frozen rotor model, compared to the unsteady calculations are robustness of the model and lower demand for computer resources. Steady state calculations can't capture unfortunately all interaction effects with complete fidelity.

Figure 8 shows the velocity field at shut off flow (Q = 0) near the volute tongue.

One can see the deceleration at the outlet of volute and the separation of the flow on the tongue of volute.

Asymmetrical pressure distribution at the outlet of impeller produces not only the radial force and its bending moment acting on the shaft, but it also

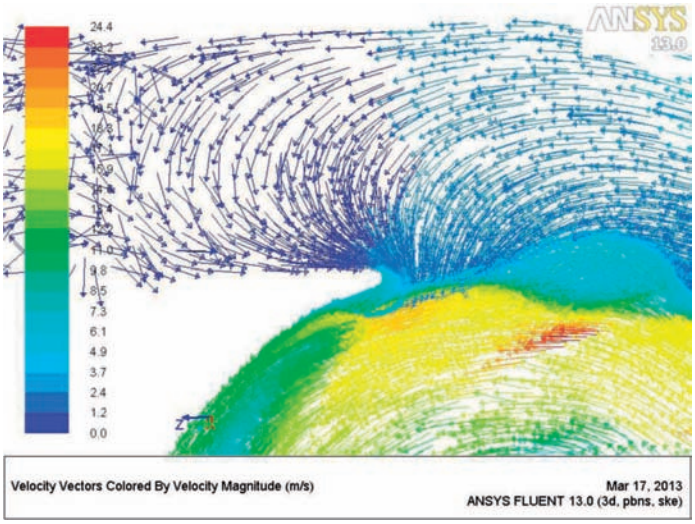

Fig. 8. Velocity field near the volute tongue at $Q = 0$

moves the axial thrust centre off the impeller axis, what creates an additional bending moment. Pressure asymmetry at the impeller outlet has an impact on the impeller sidewall gaps (Fig. 9) so one can expect that the moments of axial thrust and radial thrust have similar form.

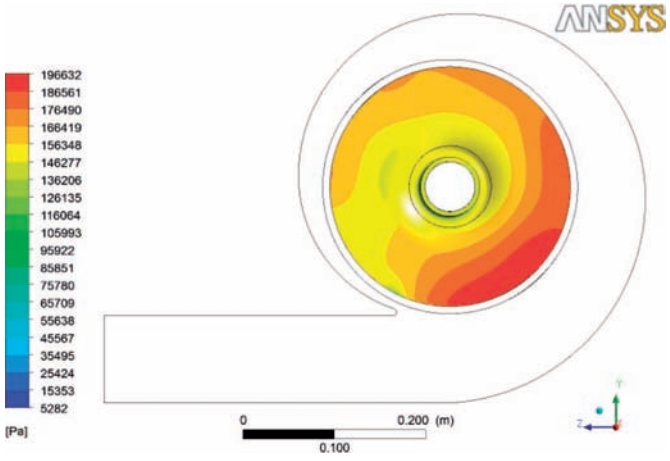

Fig. 9. Static pressure distribution on rear shroud of impeller

This interesting correlation between both distributions is presented in Fig. 10 for the rotational speed of $n = 1450$ rpm.

The presented data are in dimensionless form related to their maximum values for shut off flow. The phenomenon of axial thrust moment is usually ignored by pump designers when analyzing shaft stresses. Luckily, this moment is opposite to the radial force moment, so it lessens the shaft load.

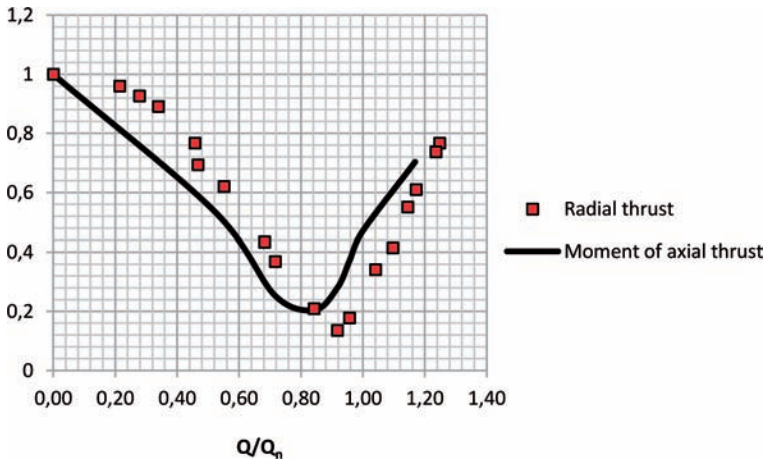

Fig. 10. Comparison between radial thrust and axial thrust moment for rotational speed 1450 rpm

One could expect similar characteristics of the radial force, since it depends on rotational speed for the same impeller geometry. Figure 11 presents distributions of force coefficient against flow coefficient for five different rotational speeds.

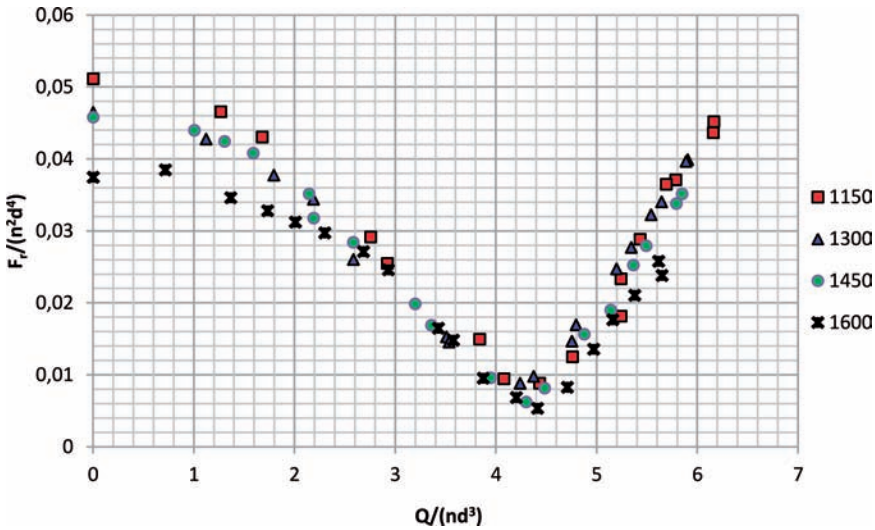

Fig. 11. Force coefficient distributions for five rotational speeds

For rotational speeds equal to or less than nominal speed, the similarity law is quite well satisfied. The discrepancy appears at highest rotational speed for low flow coefficients and is caused by higher losses connected with higher speeds.

The components of radial force showing the force direction are presented in Fig. 12.

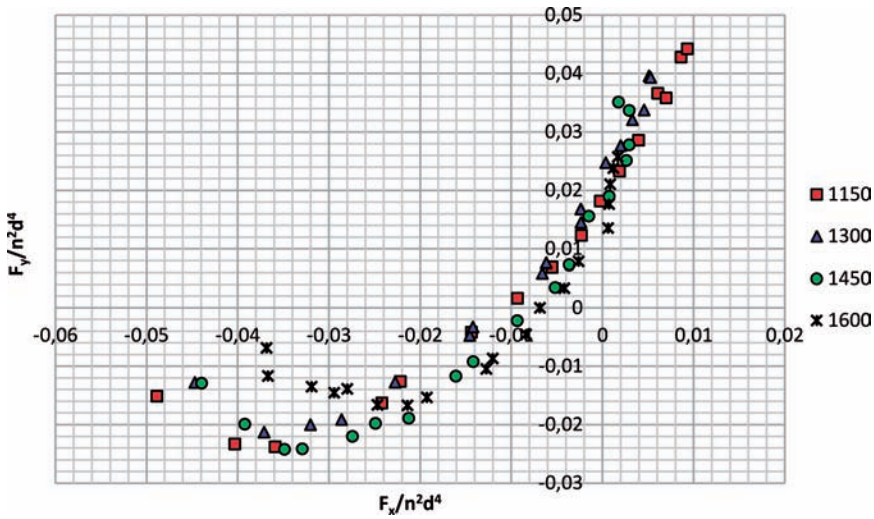

Fig. 12. The direction of measured radial force

The discrepancies appear (as previously) at highest rotational speed for low flows, due to the same reasons as mentioned above.

4. Conclusion

1. This paper presents results of radial thrust measurements for centrifugal pump of specific speed $n_s = 26$ with volute of a rectangular cross-section for several rotational speeds.
2. The results show that similarity of radial forces can be used to achieve valuable information of radial thrust for pumps with speed control. In the case of pump operating with speeds higher than nominal one, true radial thrust is lower than that estimated from the similarity law, so the predictions are on the safe side.
3. CFD with the frozen rotor scheme predicts with sufficient accuracy magnitude of radial thrust in the whole range of flows. When pump operates in the narrow range around nominal flow, optimization of pump designing is possible.
4. The frozen rotor approach may be the reason for erroneous prediction of the radial force direction. Therefore, several rotor positions should be calculated, and the results averaged for performance prediction, or predictions of one impeller position should be used as a starting point for a transient sliding-mesh simulation.
5. There is a correlation between distributions of radial force and axial thrust moment. It results from asymmetry of pressure distribution around the

impeller, which causes asymmetry of the pressure field acting on the front shroud of the impeller.

Manuscript received by Editorial Board, April 08, 2013;
final version, March 06, 2014.

REFERENCES

[1] Karassik I., Messina J., Cooper P., Heald C.: *Pump Handbook*, Fourth Edition, McGraw-Hill Prof., 2008.
[2] Stepanoff A. J.: *Centrifugal and Axial Flow Pumps: Theory, Design, and Application*, John Wiley & Sons, 1957 also Krieger Publishing Company, 1992.
[3] Agostinelli A., Nobles D., Mockridge C. R.: *An Experimental Investigation of Radial Thrust in Centrifugal Pumps*, ASME J. Eng. Power, 80, 1960, pp. 120-126.
[4] Biheller H. J.: *Radial Forces on the Impeller of Centrifugal Pumps with Volute, Semivolute, and Fully Concentric Casings*, ASME J. Eng. Power, 85, 1965, pp. 319-323.
[5] *Hydraulic Institute Standards For Centrifugal, Rotary & Reciprocating Pumps*, twelfth edition, 1969, Hydraulic Institute, New York, N. Y.
[6] *Hydraulic Institute Standards for Centrifugal, Rotary & Reciprocating Pumps*, Hydraulic Institute, Parsippany, N.J, 2009.

Badania doświadczalne i obliczenia numeryczne sił promieniowych działających na wirnik pompy odśrodkowej

Streszczenie

W artykule przedstawiono wyniki pomiarów i obliczeń naporu osiowego w pompie odśrodkowej o wyróżniku szybkobieżności n_s = 26. W badanej pompie została zastosowana spirala zbiorcza o przekroju prostokątnym. Badania wykonano dla kilku prędkości obrotowych, w tym powyżej i poniżej nominalnej. W obliczeniach wykorzystano kod ANSYS Fluent. Oprócz obliczeń siły promieniowej, zostały przeprowadzone obliczenia naporu osiowego oraz stwierdzono obecność korelacji między obiema siłami. W zakresie mierzonych prędkości obrotowych zbadane zostało również podobieństwo sił promieniowych.